Self-powered proton detectors based on GaN core–shell p–n microwires

D. Verheij, M. Peres, S. Cardoso, L. Alves, E. Alves, C. Durand, J. Eymery, J. Fernandes, K. Lorenz

Self-powered proton detectors based on GaN core-shell p-n microwires

D. Verheij,[1,2] M. Peres,[2] S. Cardoso,[1] L. C. Alves,[3] E. Alves,[2] C. Durand,[4] J. Eymery,[5] J. Fernandes,[6] and K. Lorenz[1,2]

[1)]*Instituto de Engenharia de Sistemas e Computadores - Microsistemas e Nanotecnologia (INESC- MN), Rua Alves Redol 9, 1000-029 Lisboa, Portugal*

[2)]*IPFN, Instituto Superior Técnico (IST), Campus Tecnológico e Nuclear, Estrada Nacional 10, 2695-066 Bobadela LRS, Portugal*[a)]

[3)]*C2TN, Instituto Superior Técnico (IST), Campus Tecnológico e Nuclear, Estrada Nacional 10, 2695-066 Bobadela LRS, Portugal*

[4)]*Université Grenoble Alpes, CEA, IRIG, PHELIGS, NPSC, 17 avenue des Martyrs, 38000 Grenoble, France*

[5)]*Université Grenoble Alpes, CEA, IRIG, MEM, NRS, 17 avenue des Martyrs, 38000 Grenoble, France*

[6)]*Instituto de Engenharia de Sistemas e Computadores – Investigação e Desenvolvimento (INESC-ID), Rua Alves Redol 9, 1000-029, Lisboa, Portugal*

(Dated: 12 April 2021)

Self-powered particle detectors have the potential to offer exceptional flexibility and compactness in applications where size limits and low power consumption are key requisites. Here, we report on the fabrication and characterization of radiation sensors based on GaN core/shell p-n junction microwires working without externally applied bias. With their small size, high resistance to radiation and high crystalline quality, GaN microwires constitute highly interesting building blocks for radiation-hard devices. Through microfabrication steps, single-wire devices were processed that show a leakage current as low as 1 pA in reverse bias. Irradiation with both UV light and 2 MeV protons results in photo/ionocurrent signals several orders of magnitude above the dark current and response times below 30 ms. The sensor also showed good resistance to radiation. Although we observed a small increase in the leakage current after prolonged proton irradiation, the measured transient ionocurrent signal remains stable during irradiation with a total proton fluence of at least 1×10^{16} protons/cm^2.

Self-powered radiation detectors based on wide bandgap semiconductors have attracted much interest due to their ability to detect radiation without applied bias, operation at high temperatures and blindness to radiation in the visible spectrum.[1–5] Among the wide bandgap semiconductors, GaN is well known for its high resistance to ionizing radiation owed, among other properties, to the large displacement energies of its atoms in the crystal lattice (109 eV for N and 45 eV for Ga)[6] and strong dynamic annealing effects, wherefore it is a strong candidate to be used as material for ionizing radiation detectors.[7–13] The range of radiation to which GaN is sensitive is extensive[14] and recently GaN has been used to develop self-powered UV and X-ray detectors.[15–18] Development of growth techniques for GaN also led to fabrication of high quality 1D structures, such as nano- and microwires.[19,20] This mitigates the issue of poor quality GaN films caused by lattice mismatch with the typical growth substrates to a great extent as in the case of nano- and microwires the dislocations are bent to the sidewall surface very close to the bottom, making them essentially dislocation free.[21] Additionally, wire structures possess distinctive properties such as a large surface to volume ratio and the possibility to be integrated in a flexible device.[22,23] Merging these characteristics with self-powering potential, allows fabrication of reliable, flexible and light weight detectors that can have impact in space and medical applications.

Recently, we demonstrated proton detection with radiation sensors based on n-type GaN microwires.[24,25] Although showing good sensitivity and high absolute current signals, the long decay time and persistent ionocurrent as well as the fast decrease of the conductivity due to damage induced by the radiation are relevant setbacks.[24] Shifting from a conductive device to p-n junction based detectors leads to much faster response times as has been demonstrated in UV detectors based on GaN p-n junction microwires,[26] however, no such studies have been done using ionizing radiation.

In this work, we present a study of GaN core-shell p-n junction microwires and analyze their capability to detect UV light and protons in self-powered mode. Single wire devices are microfabricated by depositing contacts at the extremities by laser photolithography and sputtering procedures. The electrical current in dark environment and under UV/proton irradiation is examined. Compared to previously studied n-type devices, the detectors show an impressive improvement in response time and improved resistance to ionizing radiation, paired with low leakage currents and good photo/iono-to-dark current ratios.

Figure 1 a) shows a scanning electron microscopy (SEM) image of the as-grown wires, vertically aligned on their growth substrate. The wires are grown by catalyst-free metal organic vapor phase epitaxy (MOVPE) on a sapphire substrate.[20] Predeposition of a SiN_x layer is followed by GaN seed nucleation by injecting trimethylgallium and ammonia at 1040 °C under a N_2 carrier gas flow. During the first stage of growth, a silane flux (200 nmol/min) is added to ensure vertical growth which simultaneously induces a heavy n-type Si doping with a donor concentration of $\sim 10^{20}$ cm^{-3}.[27] After

[a)]Electronic mail: dirkjanverheij@ctn.tecnico.ulisboa.pt

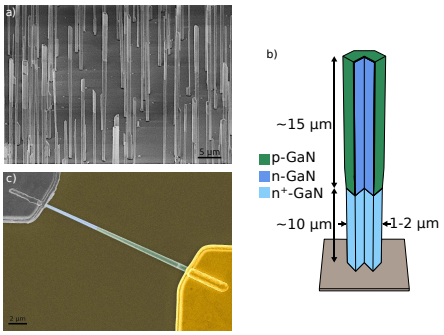

FIG. 1. a) 45 degree SEM image of as-grown wires vertically aligned on their growth substrate; b) Schematic of the structure of a single microwire; c) Top-view SEM image of a fabricated device, the thicker extremity (right) contains the p-GaN shell and the thinner part (left) is the n-GaN extremity.

$\sim$ 10 μm of vertical growth the silane flux is turned off and the GaN becomes unintentionally n-doped, now with a doping concentration of $\sim 10^{18}$ cm^{-3}.[28] Once the desired height is reached, the Mg-doped p-GaN shell is grown around the upper part of the n-type core of the microwire, creating a p-n junction in the radial direction. The shell has a thickness of $\sim$ 150 nm and is grown at 920 °C with a biscyclopentadienylmagnesium precursor followed by a dopant activation annealing performed at 750 °C for 20 minutes in a N_2 atmosphere. The doping concentration of the p-GaN shell is 10^{16}-10^{17} cm^{-3}.[28] A schematic demonstrating the configuration of a single microwire is shown in Fig. 1 b).

To allow microfabrication, the microwires were detached from their growth substrate by sonication in isopropyl alcohol and afterwards dispersed on the device substrate. TiW/Al/TiW (300/4000/150 Å) contacts were deposited at the n-GaN extremity of the wire. This deposition was followed by rapid thermal annealing at 600°C for 60 seconds to obtain an ohmic contact. Cr/Au (300/4000 Å) contacts were deposited at the p-GaN extremity of the microwire followed by rapid thermal annealing at 500°C during 60 seconds. A detailed description of the microfabrication process can be found in the supplementary material (sections I and II).

For proton irradiation, the sample was attached to a chip-carrier via a wirebonding process. 2 MeV proton irradiation was performed in a chamber allowing simultaneous Particle Induced X-ray Emission (PIXE) and electrical measurements.[29] The beam was focused to an area of 4 by 3 μm^2 and the beam current was set to 50 pA. A detailed description of the irradiation procedure can be found in the supplementary material (section IV). Photoconductivity measurements were done using a UV LED (Thorlabs M365D1, $\lambda = 365$ nm). Electrical measurements were performed with an Agilent B1500A Semiconductor Device Parameter Analyzer.

Figure 2 shows the electrical current-voltage (I-V) curves

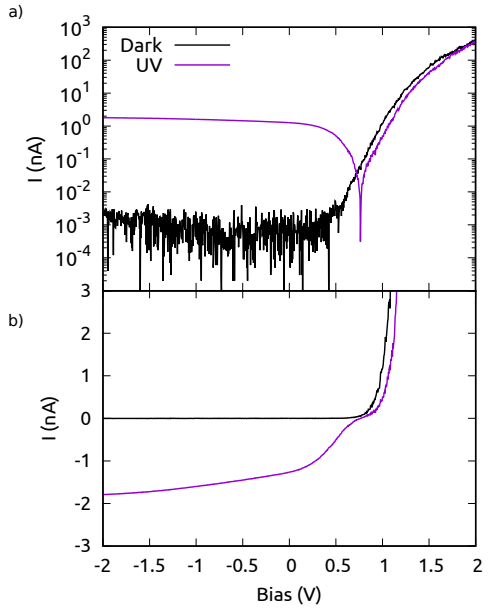

FIG. 2. I-V curve in dark and under illumination with UV light (λ = 365 nm) in logarithmic (a) and linear scale (b).

in the dark and while being illuminated with the UV LED. The sensor shows a rectifying I-V curve. In reverse bias, we observe a small leakage current around 1 pA which remains constant up to a bias of -2 volt. In forward bias, we see a rapid increase of the dark current at around 0.5 V and at 2 V the current is higher than 2 μA. Illuminating the microwire with the UV source leads to a photocurrent in the nA range in reverse bias. The photo-to-dark current ratio is above 10^3 for any bias between 0 V and -2 V. The short-circuit current is equal to 1.26 nA and the device has an open-circuit voltage of 0.76 V. The open-circuit voltages measured on other devices were all between 0.71 V and 0.78 V, values which are similar to the ones measured in previous studies.[30,31] Furthermore, we observe that the photocurrent shows a small linear growth with increasing reverse bias caused by the increase in width of the depletion region when we increase the magnitude of reverse bias. In forward bias, the dark and photocurrent are similar showing that photoconductive effects are minimized. It is also worth mentioning that the I-V curves indicate the presence of a small potential barrier at the metal-semiconductor interfaces. Where an ideal p-n junction diode has an almost constant photocurrent near zero bias which only becomes positive when the bias is high enough to flatten the potential bias of the p-n junction, the photocurrent in our device starts decreasing before this (between 0.25 and 0.85 V). In this case, the fields created by the Schottky barriers have opposite signs to the field created by the p-n junction originating a photocur-

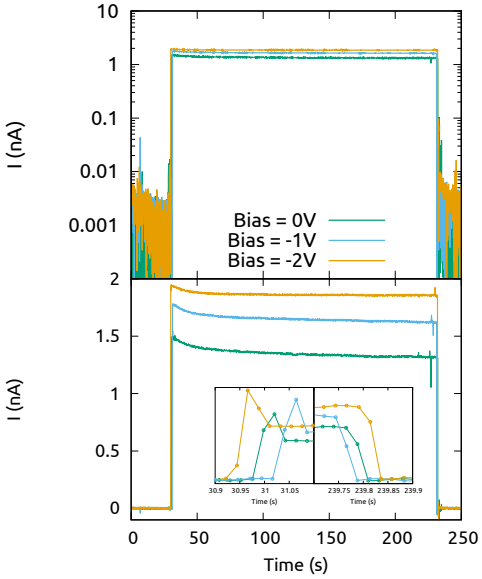

FIG. 3. Transient photoconductivity in the GaN microwire as it is exposed to a single light square pulse of UV radiation with = 365 nm at 0 V, -1 V and -2 V in logarithmic scale (a) and in linear scale (b). The inset in (b) shows the rise and decay of the photocurrent in a smaller time scale.

rent that begins to compensate the photocurrent originated in the p-n junction. However, the fact that we still observe a photocurrent larger than -1 nA at zero bias, indicates that the contribution of the p-n junction is more significant. Similar observations where made using ITO[32] and Ni/Au contacts.[33]

The transient photocurrent characteristic shown in figure 3, studied by measuring the detector response to square light pulses at different bias, allows us to analyze the interplay between the photovoltaic and photoconductive modes and the transient characteristics of the device. At zero bias we measure a photo-to-dark current ratio of approximately 10^3 while the rise and fall times are between 20 ms and 30 ms (detection limit of our measurement equipment). When we increase the bias we observe a small increase in the photocurrent while the rise and fall times remain the same. Contrarily to previous measurements made using n-type microwires, we do not observe any persistent photocurrent (PPC).[24] Finally, we estimated the responsivity of samples and obtained a maximum value of R(λ = 365 nm) $\sim$ 0.06 A/W considering the active area to be half of the total exposed surface area of the microwire (see supplement). This value is of the same order of magnitude as the value obtained in reports using similar microwires as in this study.[30,34] Additionally, we observed that the photocurrent signal has a linear response relative to the optical power of the light source and that the responsivity at 365 nm of several devices is constant (shown in the supplementary

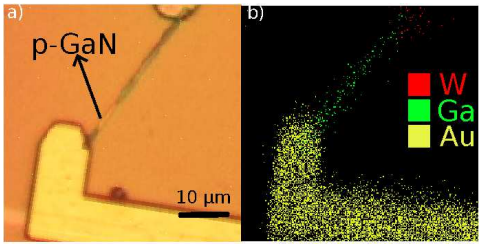

FIG. 4. a) Microscope image of the sample that was irradiated; b) 53×53 μm^2 sized PIXE map where the yellow dots correspond to counts of Au, the red dots to counts of W and the green dots to counts of Ga.

material, section III).

The main novelty of this study is to show that the good photo-to-dark current ratio and fast time characteristic of the sensor are maintained when shifting from UV radiation to ionizing radiation.

Figure 4 shows a 53×53 μm^2 sized PIXE map of the microwire (Ga-signal in green) and the contacts (Au signal in yellow, W signal in red) together with a microscope image of the sample. Using the PIXE map as a reference we can select smaller areas which allows us to study the behavior of the sensor in more detail. To distinguish between the half containing the p-n junction and the n-GaN half of the microwire we choose two small areas for the beam to scan near the respective contact regions as can be seen in the insets of figure 5. Each area has a size of roughly 10x10 μm^2. We then proceed to perform I-V measurements during the irradiation. When irradiating the p-n junction (figure 5 a)) the obtained signal is similar to the signal obtained with UV light. In reverse bias, although the ratio between the iono-to-dark current is smaller in comparison to the photo-to-dark current ratio shown above, the ionocurrent is still roughly 100 times larger than the dark current. We attribute the difference between both ratios to the distinct excitation densities and mechanisms. While UV light is absorbed close to the surface i.e. close to the depletion region, protons cross the entire wire leading to homogeneous excitation along their tracks. According to Monte Carlo simulations using the SRIM code[35], the range of protons in GaN is about 24 μm. At zero bias we measure a short-circuit current of $\sim$ 120 pA and at low positive bias the ionocurrent starts decreasing until being canceled by the forward bias current. The open-circuit voltage has a value of 0.74 V. The latter value is close to the value for UV illumination, confirming that the main difference lies in the carrier generation rate for the two different excitation processes.

We then select the smaller area that contains the n-GaN half and repeated the measurements (figure 5 b)). We note that this measurement was performed after the measurements shown in figures 5 a) and 6, consequently the sample has suffered from some radiation damage. This damage caused a slight increase in the reverse bias leakage current and decrease of the forward bias current, which explains the difference between the dark

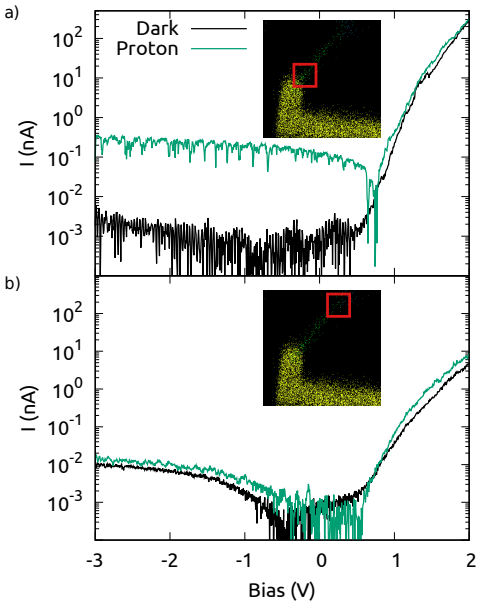

FIG. 5. I-V curve in dark and when irradiating the p-GaN extremity (a)) and when irradiating the n-GaN extremity (b)) with 2 MeV protons. The areas that are being irradiated are marked by the red squares on the PIXE map shown in the inset. The measurements in b) were performed after irradiation with a total fluence of $\sim 1.5 \times 10^{16}$ protons/cm^2

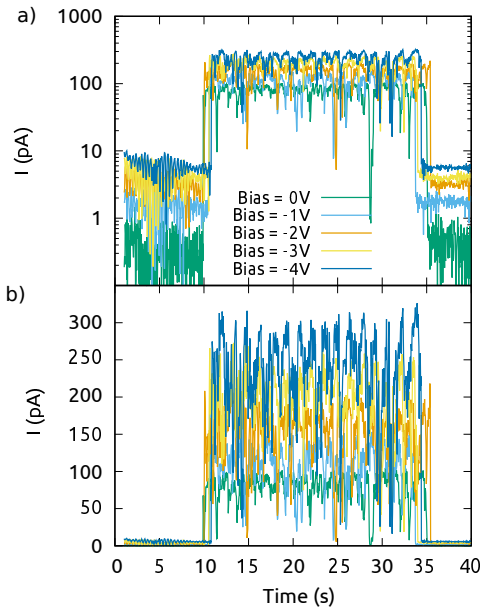

FIG. 6. Transient ionoconductivity when irradiating the p-GaN extremity (see fig.5 at 0 V, -1 V and -2 V in logarithmic (a)) and linear (b)) scale.

currents in figure 5 a) and in figure 5 b). This point is further addressed below. Regarding the behavior of the device when irradiating the n-GaN, without excitation of excess charge carriers in the depletion region of the p-n junction the signal in reverse bias is almost negligible. On the other hand, we observe an ionocurrent signal in forward bias, resulting from the charge carriers created in the n-GaN.

To take a closer look at the dependence on bias and at the transient characteristics of the ionocurrent we performed transient I-V measurements at fixed bias. For each measurement shown in figure 6, the fluence of irradiation is $\sim 2 \times 10^{15}$ protons/cm^2. The variations in the ionocurrent signal are a result of fluctuations in the beam current. Regarding the dependence of the ionocurrent on bias, we can see that the ionocurrent increases by a factor of approximately 2 from 0 V to -2 V (slightly higher than for photoconductivity measurements) and a factor of 3 from 0 V to -4 V, which we attribute to the increase of the depletion region width of the p-n junction. The differences between UV and proton irradiation, with a higher increase of the ionocurrent with bias than the photocurrent, can be attributed again to the different excitation volumes. While protons cross the entire microwire creating electron-hole pairs along their paths, UV light is absorbed close to the surface. The rise and fall times have values of approximately 25 ms and, similar to the photocurrents shown in figure 3, do not increase when applying a reverse bias. Finally, neither the ionocurrent nor the dark current after irradiation decrease during the measurements. This is contrary to what we observed when irradiating sensors based on n-type GaN wires for which irradiation causes a significant decrease of the dark current (see supplement fig. S7).

We believe that these distinct behaviors result from the different dependence of the device characteristics on the total free carrier concentration. One of the main consequences of the irradiation damage created in the GaN lattice is the removal of free carriers.[9] Consequently, even if the number of carriers created by the ion beam is the same, the total carrier concentration diminishes.This will strongly influence the total resistance of the n-type device. On the contrary, the electrical behavior of the p-n junction diode with zero or reverse bias is found to be less sensitive to these carrier traps.

Concerning the evolution of the dark current with increasing radiation fluence we observed an increase in the reverse bias leakage current as well as a decrease in the forward bias dark current. As for the leakage current, it remained unaffected after irradiating with a fluence of 6.1×10^{14} protons/cm^2 but increased by one order of magnitude after irradiating with a fluence of $\sim 2 \times 10^{16}$ protons/cm^2. Additional measurements done on similar samples (see supplement fig. S6) furthermore showed that we only observe

meaningful modification of the leakage currents for an irradiation fluence above 1×10^{15} protons/cm^2. We performed the same experiment using a commercial Si PIN diode and observed that the dark current at -2 V increased by more than three orders of magnitude after irradiation with a fluence of 1×10^{15} protons/cm^2. A direct comparison of these values is not straight forward due to the different geometries of the devices. Nevertheless, they give a good indication of the superior radiation resistance of GaN-based devices compared to Si devices.

Regarding the decrease of the forward bias conductivity, we attribute this to the increase of the total resistivity of the sample that occurs when radiation induced defects are created. Prior research on the influence of proton irradiation on GaN diodes based on bulk crystals and heteroepitaxial thin films have shown similar results. King et al. irradiated a vertical GaN PIN diode with 2.5 MeV protons and saw increased leakage for a reverse bias larger than -900 V at a proton fluence of 3.1×10^{13} protons/cm^2.[36] For lower biases they did not observe any measurable changes up to this fluence. Moreover, the evolution of the short-circuit current as a function of the proton fluence of radiation sensors based on GaN LED structures was studied by Gaubas et al..[37] They observed that the short-circuit current decreased significantly for 1.6 MeV proton fluences above 1×10^{15} protons/cm^2. Our transient measurements shown in figure 6 suggest stability of our device up to a fluence of at least 1×10^{16} protons/cm^2. However, we should take care when comparing our results with these studies due to the unique structure and dimensions of our samples. Nevertheless, the stability of the ionocurrent and small increase in reverse bias leakage are promising results that confirm the good resistance to radiation of our devices.

In summary, we have demonstrated that GaN core-shell p-n microwires can be used as radiation sensors, identifying them as potential building blocks for self-powered ionizing radiation detectors by showing a good iono-to-dark current ratio and fast response times at zero bias. The radial depletion region created by the p-n junction separates the created charge carriers which are afterwards collected by the electrodes deposited at the extremities of the wires. Despite being exposed to a relatively high proton flux, the signal of the sensors does not decrease when irradiating the device for a considerable time period. In addition, the leakage current in reverse bias remained constant in all studied devices up to a fluence of $\sim 1 \times 10^{15}$ protons/cm^2 and it showed moderate increase after proton irradiation with a fluence of $\sim 2 \times 10^{16}$ protons/cm^2. This kind of detectors can be applied in several areas where size and self-powering characteristics are important, namely space and medical applications. A specific example where GaN microwire based radiation sensors can be applied is the field of *in-vivo* dose monitoring during brachytherapy.[38]

See the supplementary material for more information about the microfabrication process, photoconductivity measurements and description of the proton irradiation and measurements.

The authors wish to acknowledge funding by the Fundação para a Ciência e a Tecnologia (FCT) (PTDC/CTM-CTM/28011/2017, LISBOA-01-0145-FEDER-028011, UID/05367/2020, UIDB/04349/2020, DV thanks FCT for his grant PD/BD/143015/2018 within the AIM doctoral program). Research was supported by the EU H2020 project no. 824096 "RADIATE".

The data that supports the findings of this study are available within the article and its supplementary material. Further details regarding the data are available from the corresponding author upon reasonable request.

[1] Y. Yang, W. Guo, J. Qi, J. Zhao, and Y. Zhang, Appl. Phys. Lett. **97**, 223113 (2010).
[2] Y. Q. Bie, Z. M. Liao, H. Z. Zhang, G. R. Li, Y. Ye, Y. B. Zhou, J. Xu, Z. X. Qin, L. Dai, and D.-P. Yu, Advanced Materials **23**, 649 (2011).
[3] S. Yang, S. Tongay, S. S. Li, J. B. Xia, J. Wu, and J. Li, Appl. Phys. Lett. **103**, 143503 (2013).
[4] Z. Chen, B. Li, X. Mo, S. Li, J. Wen, H. Lei, Z. Zhu, G. Yang, P. Gui, F. Yao, and G. Fang, Appl. Phys. Lett. **110**, 123504 (2017).
[5] R. Dahal, K. C. Huang, J. Clinton, N. LiCausi, J. Q. Lu, Y. Danon, and I. Bhat, Applied Physics Letters **100**, 243507 (2012).
[6] J. Nord, K. Nordlund, J. Keinonen, and K. Albe, Nucl. Instrum. Methods Phys. Res. B **202**, 93 (2003).
[7] S. J. Pearton, R. Deist, F. Ren, L. Liu, A. Y. Polyakov, and J. Kim, J. Vac. Sci. Technol. A **31**, 050801 (2013).
[8] S. J. Pearton, F. Ren, E. Patrick, M. E. Law, and A. Y. Polyakov, ECS J. Solid State Sci. and Technol. **5**, Q35 (2015).
[9] A. Y. Polyakov, S. J. Pearton, P. Frenzer, F. Ren, L. Liu, and J. Kim, J. Mater. Chem. C **1**, 877 (2013).
[10] J. Marques, K. Lorenz, N. Franco, and E. Alves, Nucl. Instrum. Methods Phys. Res. B **249**, 358 (2006).
[11] K. Lorenz, M. Peres, N. Franco, J. G. Marques, S. M. C. Miranda, S. Magalhães, T. Monteiro, W. Wesch, E. Alves, and E. Wendler, Proc. SPIE **7940**, 79400O (2011).
[12] K. Lorenz, E. Wendler, A. Redondo-Cubero, N. Catarino, M.-P. Chauvat, S. Schwaiger, F. Scholz, E. Alves, and P. Ruterana, Acta Materialia **123**, 177 (2017).
[13] M. C. Sequeira, J. G. Mattei, H. Vazques, F. Djurabekova, K. Nordlund, I. Monnet, P. Mota-Santiago, P. Kluth, C. Grygiel, S. Zhang, E. Alves, and K. Lorenz, Commun Phys **4**, 51 (2021).
[14] J. Wang, P. Mulligan, L. Brillson, and L. R. Cao, Appl. Phys. Rev. **2**, 031102 (2015).
[15] A. V. Babichev, H. Zhang, P. Lavenus, F. H. Julien, A. Y. Egorov, Y. T. Lin, L. W. Tu, and M. Tchernycheva, Appl. Phys. Lett. **103**, 201103 (2013).
[16] W. Song, X. Wang, H. Chen, D. Guo, M. Qi, H. Wang, X. Luo, X. Luo, G. Li, and S. Li, J. Mater. Chem. C **5**, 11551 (2017).
[17] N. A. A. Zulkifli, K. Park, J.-W. Min, B. S. Ooi, R. Zakaria, J. Kim, and C. L. Tan, Appl. Phys. Lett. **117**, 191103 (2020).
[18] L. Zhou, X. Lu, J. Wu, H. Jiang, L. Chen, X. Ouyang, and K. M. Lau, IEEE Electron Device Letters **40**, 1044 (2019).
[19] R. Songmuang, O. Landré, and B. Daudin, Appl. Phys. Lett. **91**, 251902 (2007).
[20] R. Koester, J. S. Hwang, C. Durand, D. L. S. Dang, and J. Eymery, Nanotechnology **21**, 015602 (2009).
[21] P. M. Coulon, M. Mexis, M. Teisseire, M. Jublot, P. Vennéguès, M. Leroux, and J. Zuniga-Perez, J. Appl. Phys. **115**, 153504 (2014).
[22] X. Dai, A. Messanvi, H. Zhang, C. Durand, J. Eymery, C. Bougerol, F. H. Julien, and M. Tchernycheva, Nano Letters **15**, 6958 (2015).
[23] H. Zhang, X. Dai, N. Guan, A. Messanvi, V. Neplokh, V. Piazza, M. Vallo, C. Bougerol, F. H. Julien, A. Babichev, N. Cavassilas, M. Bescond, F. Michelini, M. Foldyna, E. Gautier, C. Durand, J. Eymery, and M. Tchernycheva, ACS Appl. Materials Interfaces **8**, 26198 (2016).
[24] D. Verheij, M. Peres, S. Cardoso, L. C. Alves, E. Alves, C. Durand, J. Eymery, and K. Lorenz, J. Phys. D: Appl. Phys. **51**, 175105 (2018).
[25] D. Verheij, M. Peres, S. Cardoso, L. C. Alves, E. Alves, C. Durand, J. Eymery, J. Fernandes, and K. Lorenz, EPJ Web Conf. **233**, 05001 (2020).
[26] H. Zhang, A. Messanvi, C. Durand, J. Eymery, P. Lavenus, A. Babichev, F. H. Julien, and M. Tchernycheva, Phys. status solidi A **213**, 936 (2016).
[27] P. Tchoulfian, F. Donatini, F. Levy, B. Amstatt, A. Dussaigne, P. Ferret, E. Bustarret, and J. Pernot, Appl. Phys. Lett. **103**, 202101 (2013).

[28]P. Tchoulfian, F. Donatini, F. Levy, A. Dussaigne, P. Ferret, and J. Pernot, Nano Letters **14**, 3491 (2014).
[29]M. Peres, L. C. Alves, F. Rocha, N. Catarino, C. Cruz, E. Alves, A. G. Silva, E. G. Víllora, K. Shimamura, and K. Lorenz, Phys. status solidi (a) **215**, 1800190 (2018).
[30]H. Zhang, N. Guan, V. Piazza, A. Kapoor, C. Bougerol, F. H. Julien, A. V. Babichev, N. Cavassilas, M. Bescond, F. Michelini, M. Foldyna, E. Gautier, C. Durand, J. Eymery, and M. Tchernycheva, J. of Phys. D: Appl. Phys. **50**, 484001 (2017).
[31]A. Messanvi, H. Zhang, V. Neplokh, F. H. Julien, F. Bayle, M. Foldyna, C. Bougerol, E. Gautier, A. Babichev, C. Durand, J. Eymery, and M. Tchernycheva, ACS Appl. Mat. Interfaces **7**, 21898 (2015).
[32]G. Jacopin, A. De Luna Bugallo, L. Rigutti, P. Lavenus, F. H. Julien, Y.-T. Lin, L.-W. Tu, and M. Tchernycheva, Appl. Phys. Lett. **104**, 023116 (2014).
[33]P. Lavenus, A. Messanvi, L. Rigutti, A. D. L. Bugallo, H. Zhang, F. Bayle, F. H. Julien, J. Eymery, C. Durand, and M. Tchernycheva, Nanotechnology **25**, 255201 (2014).
[34]M. Tchernycheva, A. Messanvi, A. de Luna Bugallo, G. Jacopin, P. Lavenus, L. Rigutti, H. Zhang, Y. Halioua, F. H. Julien, J. Eymery, and C. Durand, Nano Letters **14**, 3515 (2014).
[35]J. F. Ziegler, M. Ziegler, and J. Biersack, Nucl. Instrum. Methods Phys. Res. B **268**, 1818 (2010).
[36]M. P. King, A. M. Armstrong, J. R. Dickerson, G. Vizkelethy, R. M. Fleming, J. Campbell, W. R. Wampler, I. C. Kizilyalli, D. P. Bour, O. Aktas, H. Nie, D. Disney, J. Wierer, A. A. Allerman, M. W. Moseley, F. Leonard, A. A. Talin, and R. J. Kaplar, IEEE T. Nucl. Sci. **62**, 2912–2918 (2015).
[37]E. Gaubas, T. Čeponis, D. Meškauskas, J. Pavlov, A. Žukauskas, V. Kovalevskij, and V. Remeikis, Sens. Actuat. A Phys. **267**, 194 (2017).
[38]K. Tanderup, S. Beddar, C. E. Andersen, G. Kertzscher, and J. E. Cygler, Medical Physics **40**, 070902 (2013).

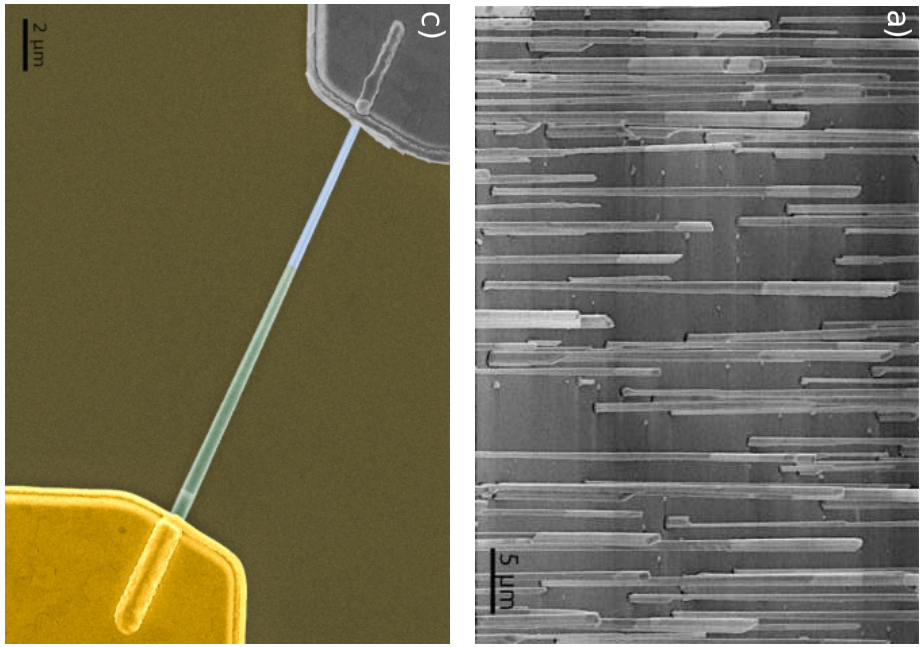

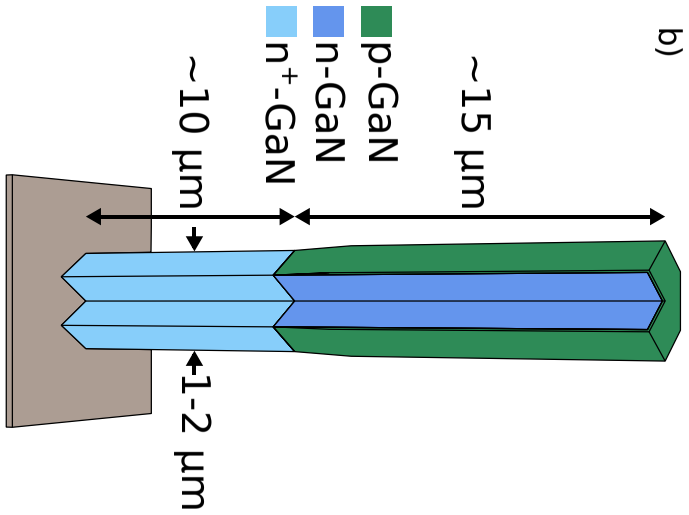

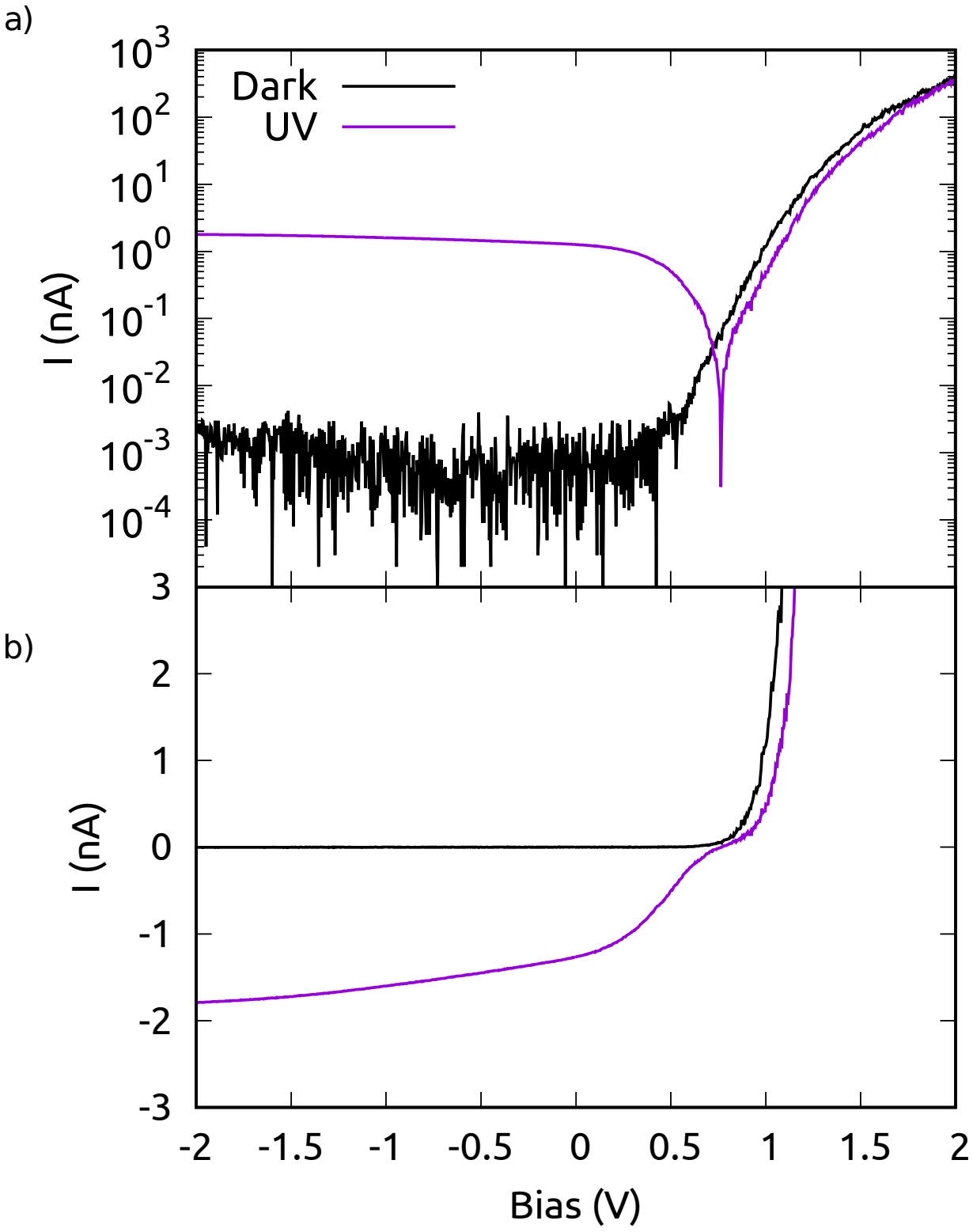

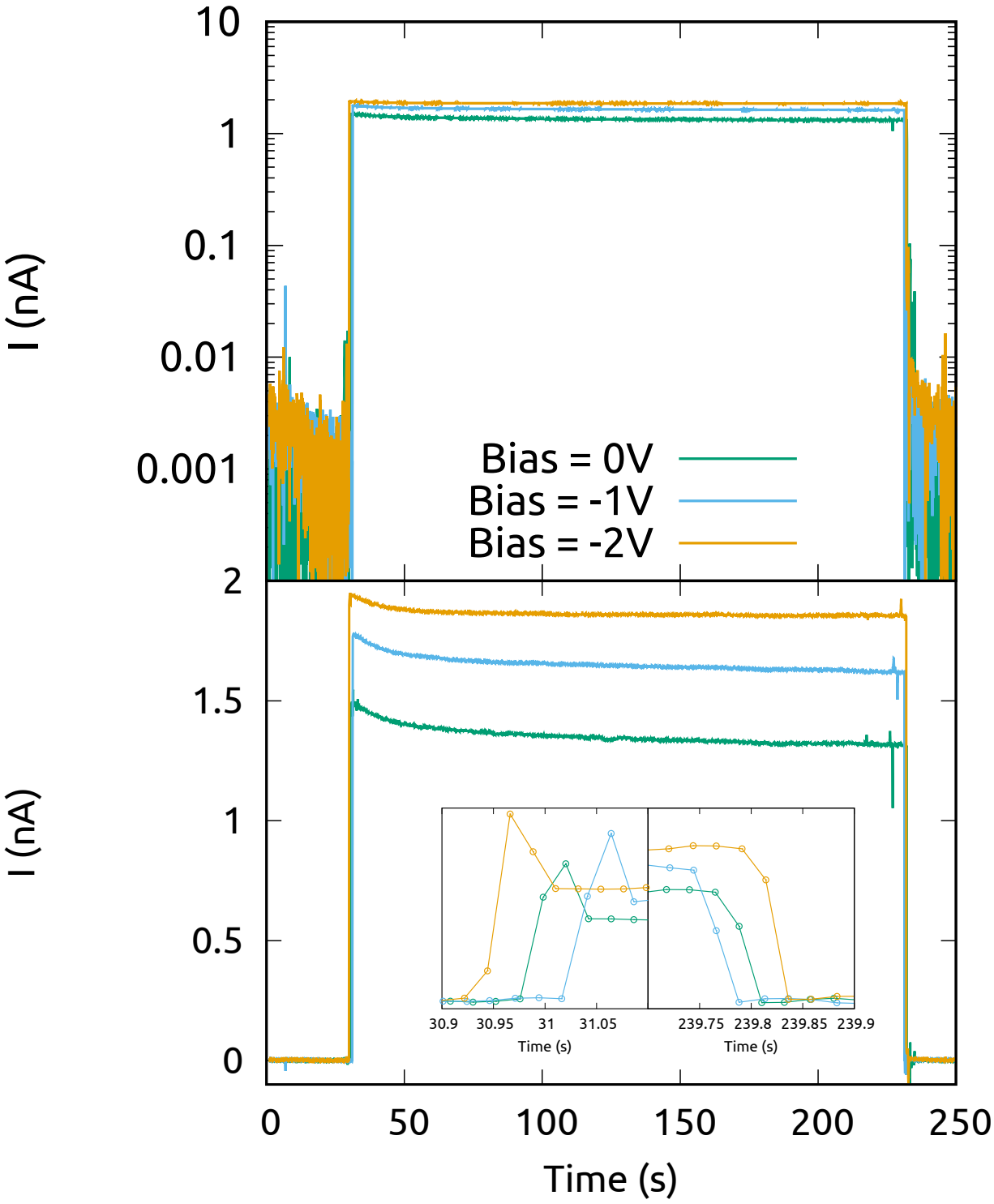

PLEASE CITE THIS ARTICLE AS DOI: 10.1063/5.0045050